Helical Figure-of-Eight Loop Dicopper(I) Compounds: Syntheses, Structures, and Dynamics

Peter Comba,*,† Andreas Fath,† Trevor W. Hambley,‡ Andreas Kühner,† David T. Richens,§ and Annette Vielfort†

Anorganisch-Chemisches Institut der Universität, Im Neuenheimer Feld 270, D-69120 Heidelberg, School of Chemistry, The University of Sydney, NSW 2006, Australia, and Department of Chemistry, The University of St. Andrews, KY16 9ST, UK

Received February 27, 1998

The synthesis of a series of nine large macrocyclic ligands with two N_2S_2 (thioether and Schiff-base imine) binding sites each, with different bridges between the donor atoms of each site (ethylene, *o*-xylylene, propylene, butylene) and different spacer groups between the two binding sites (*p*-xylylene, 2,5-dimethyl-*p*-xylylene, 2,5-dimethoxy-*p*-xylylene), and the synthesis of a similar ligand with a preorganized double-helical geometry, based on a paracyclophane spacer group, are reported, together with the syntheses and characterizations of the corresponding dicopper(I) compounds. The solid state structures of the dicopper(I) complexes have two tetrahedral copper(I) sites, separated by ca. 8 Å, and a figure-of-eight loop configuration of the ligand with a parallel arrangement of the two substituted benzene spacer groups (benzene···benzene distance of ca. 3.5 Å). All the dicopper(I) compounds have the same double-helical configuration ("twisted ring figure-of-eight loop"). NMR spectroscopy indicates that the monocyclic metal-free ligands have an open, cyclic structure in solution, while the dicopper(I) compounds are folded as in the solid. In acetonitrile there is a fast dynamic equilibrium between two enantiomeric forms of the double-helical dicopper(I) compounds. The fact that copper(I)-donor atom bond breaking is involved in this process is supported by ^{1}H NMR data and by the X-ray crystal structure analysis of a putative intermediate with each of the two copper(I) centers coordinated to one acetonitrile and three donors of the macrocycle. A second fast dynamic, solvent independent process (epimerization) has been identified in nitromethane and acetonitrile, involving helix inversion with full conservation of the copper(I) coordination.

Introduction

Helical secondary structures are an important feature in biological systems. Helices are not only observed in proteins and DNA but also in cyclic peptides such as Cyclosporin A, Ascidiacyclamide, and Patellamide D, occurring in bacteria, fungi, plants, and marine organisms, and the unique properties of these systems as metal-free and coordinated macrocyclic ligands may partly be related to their folding.[1] Therefore, it is not surprising that helical transition metal compounds have attracted considerable attention in recent years, and their shape and intrinsic chirality, as well as features related to self-assembly, supramolecular properties, and their relevance to biological systems and in material science have been studied and reviewed extensively.[2] The majority of transition metal compounds studied in this field are based on polypyridine type ligands,[3] and few systems with other donor sets have been reported.

Recently, macrocyclic Schiff-base ligands with $(N_2S_2)_2$ (thioether and imine) donor sets were reported which, depending on the ligand, show copper(I)-induced figure-of-eight loop folding: ligands with para-substituted benzene spacer groups lead to a chiral double-helical configuration ("twisted ring figure-of-eight loop") while those with meta-substituted spacer groups lead to a structurally related but achiral folding ("squeezed ring figure-of-eight loop"); the structure of the dicopper(I) compound of a preorganized helical ligand has also been reported (see Scheme 1).[4]

We now describe in detail the syntheses of a variety of this type of ligand and the corresponding dicopper(I) compounds

* Corresponding author. Fax: +49 6221 546 617. E-mail: comba@akcomba.oci.uni-heidelberg.de.

† Universität Heidelberg.

‡ The University of Sydney.

§ University of St. Andrews.

(1) (a) Lewis, J. R. *Nat. Prod. Rep.* **1989**. (b) Rosen, M. K.; Schreiber, S. L. *Angew. Chem., Int. Ed. Engl.* **1992**, *31*, 384. (c) Fusetani, N.; Sugawara, T.; Matsunaga, S. *J. Am. Chem. Soc.* **1991**, *113*, 7811. (d) Schmitz, F. J.; Ksebati, M. B.; Cheng, J. S.; Wang, J. L.; Hossain, M. B.; van der Helm, D.; Engel, M. H.; Serban, A.; Silfer, J. A. *J. Org. Chem.* **1989**, *54*, 3463. (e) Michael, J. P.; Pattenden, G. *Angew. Chem., Int. Ed. Engl.* **1995**, *34*, 1883. (f) van den Brenk, A.; Byriel, K. A.; Fairlie, D. P.; Gahan, L. R.; Hanson, G. R.; Hawkins, C. J.; Jones, A.; Kennard, C. H. L.; Murray, K. S. *Inorg. Chem.* **1994**, *33*, 3549. (g) van den Brenk, A.; Fairlie, D. P.; Gahan, L. R.; Hanson, G. R.; Hambley, T. W. *Inorg. Chem.* **1996**, *35*, 1059.

(2) (a) Constable, E. C. *Nature (London)* **1990**, *346*, 314. (b) Sauvage, J. P. *Acc. Chem. Res.* **1990**, *23*, 319. (c) Lehn, J.-M. *Angew. Chem.* **1990**, *102*, 1347; *Angew. Chem., Int. Ed. Engl.* **1990**, *29*, 1304. (d) Constable, E. C. *Chem. Ind. (London)* **1994**, 56. (e) Piguet, C.; Bernadelli, G.; Hopfgartner, G. *Chem. Rev.* **1997**, 97, 2005−2062.

(3) (a) Koert, U.; Harding, M. M.; Lehn, J.-M. *Nature (London)* **1990**, *346*, 339. (b) Zarges, W.; Hall, J.; Lehn, J.-M. *Helv. Chim. Acta* **1991**, *74*, 1843. (c) Judice, J. K.; Keipert, S. J.; Cram, D. J. *J. Chem. Soc., Chem. Commun.* **1993**, 1323. (d) Potts, K. T.; Keshavarz-K, M.; Tham, F. S.; Abruña, H. D.; Arana, C. *Inorg. Chem.* **1993**, *32*, 4436. (e) Krämer, R.; Lehn, J.-M.; De Cian, A.; Fischer, J. *Angew. Chem.* **1993**, *105*, 764; *Angew. Chem., Int. Ed. Engl.* **1993**, *32*, 703. (f) Constable, E. C.; Edwards, A. J.; Raithby, P. R.; Walker, J. V. *Angew. Chem.* **1993**, *105*, 1486; *Angew. Chem., Int. Ed. Engl.* **1993**, *32*, 1465. (g) Bilyk, A.; Harding, M. M. *J. Chem. Soc., Dalton Trans.* **1994**, 77.

(4) (a) Comba, P.; Fath, A.; Hambley, T. W.; Richens, D. T. *Angew. Chem., Int. Ed. Engl.* **1995**, *34*, 1883. (b) Comba, P.; Fath, A.; Hambley, T. W.; Vielfort, A. *J. Chem. Soc., Dalton Trans.* **1997**, 1691. (c) Comba, P.; Fath, A.; Huttner, G.; Zsolnai, L. *J. Chem. Soc., Chem. Commun.* **1996**, 1885. (d) Comba, P.; Kühner, A. Submitted. (e) Wei G.; Lawrance G. A.; Richens D. T.; Hambley T. W.; Turner P. *J. Chem. Soc., Dalton Trans.* **1998**, 623. (f) Comba, P.; Kühner, A.; Peters, A. Submitted.

S0020-1669(98)00216-X CCC: $15.00
Published on Web 08/24/1998

Scheme 1[a]

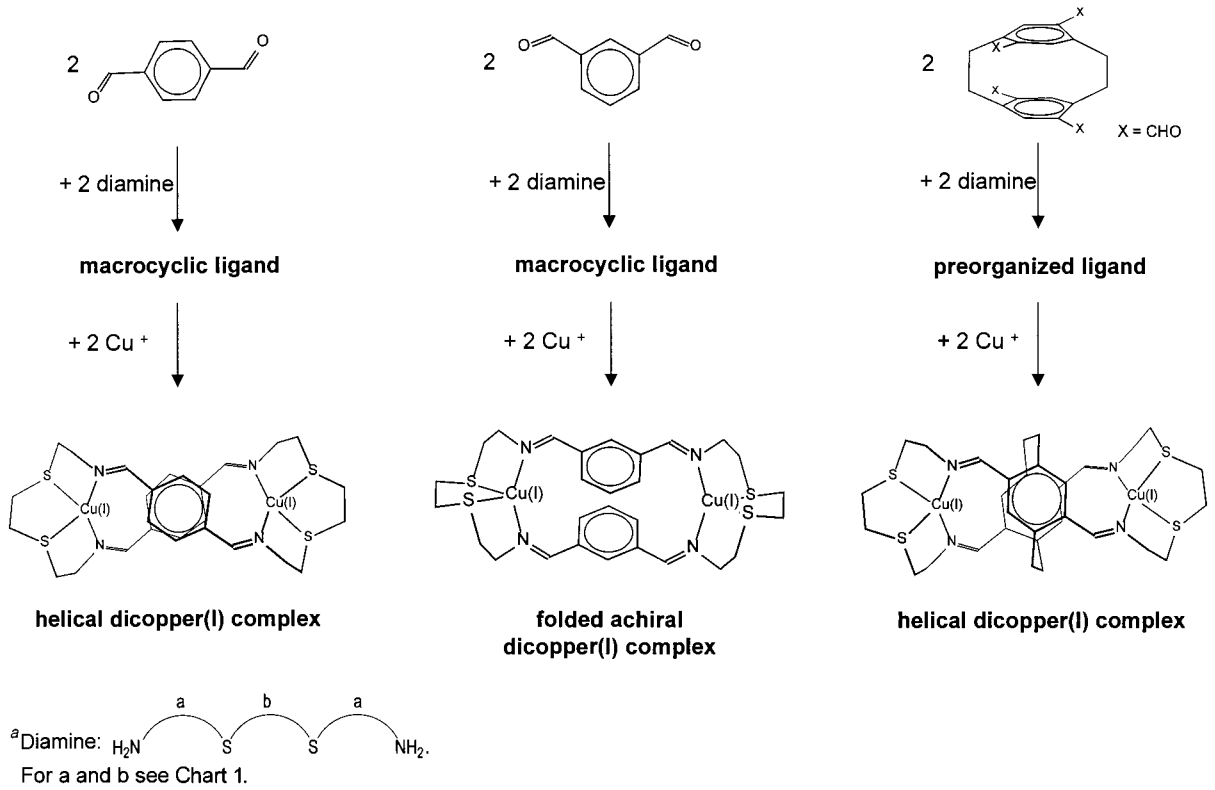

(see Chart 1; the synthesis and structure of the dicopper(I) compound with the meta-substituted benzene spacer groups has been reported,[4b] and its detailed solution properties will be discussed in a separate publication[4d]). The structural properties are discussed on the basis of X-ray crystal structural analyses and solution ^{1}H NMR spectroscopic measurements. In solution, two dynamic processes have been identified: the first is solvent independent and involves the inversion of the helices with full conservation of the coordination to the two metal centers, and the second occurs in acetonitrile and involves the unfolding of the macrocyclic ligand complexes (bond breaking promoted by the coordination of solvent molecules). The interpretation for the latter process is supported by the experimentally determined structure of a putative intermediate.

Results and Discussion

Syntheses, Electronic Spectroscopy, and Electrochemistry. The preparation of the macrocyclic ligands is based on a well-documented and generally high-yielding [2+2] condensation reaction,[5] and that of the preorganized ligand with the paracyclophane anchor group involves a novel but similar [1+2] condensation that yields the white solid in 70−80%.[4c] The tetraformyl precursor for the latter synthesis is obtained by a Bouveault reaction, involving lithiation of the corresponding, known *trans*-tetrabromoparacyclophane,[6] followed by reaction with dimethylformamide and acid hydrolysis.[4c] The yellow or yellow-orange dicopper(I) complexes are generally obtained by addition of a $[Cu(NCCH_3)_4]ClO_4$ solution to the ligand solution, and crystals suitable for X-ray structural analyses were isolated after slow evaporation of the solvent from the clear solutions. All dicopper(I) compounds reported here are moderately soluble in acetonitrile and in nitromethane. Samples of the solids are stable when exposed to air and humidity (for several months (double-helical structures, see below) or several days), solutions in acetonitrile are generally more stable than those in nitromethane.

The UV−vis spectra of the dicopper(I) complexes are dominated by a transition around 350 nm with a moderately high intensity (ca. 4000 $dm^3\ mol^{-1}\ cm^{-1}$; see Table 1), tentatively assigned to a metal-to-ligand charge-transfer transition (MLCT),[4b] and signals between 200 and 350 nm with higher intensities (up to 70 000 $dm^3\ mol^{-1}\ cm^{-1}$), tentatively assigned to intraligand transitions.[4b] As expected, there is a qualitative correlation between the energy of the putative MLCT transition (low-energy electronic transition) and the stability of the double-helical structure (the thermodynamic stability of the dicopper-(I) compounds is also related to the stability of the helical structures, see section on dynamics below). However, due to the number of parameters that are varied in the eight compounds reported here (size of chelate rings, substituents on the benzene spacer groups, substituents on the chelate rings), a more than qualitative interpretation is not warranted.

Electrochemical data of the dicopper(I) compounds have been obtained from dilute solutions in nitromethane and acetonitrile (Table 2). Generally, a single reversible reduction wave is observed, indicating that, as expected from the copper−copper distance of ca. 8 Å, there is no metal···metal interaction.[4] Addition of ferrocene has in these systems generally a strong effect on the cyclovoltamograms. This is attributed to the effects of a monolayer of ferrocene at the electrode surface.[4e] The effect of the substituents to the benzene spacer groups (H vs Me vs OMe; first three entries in Table 2) is similar in both solvents and similar to the effects seen in the electronic spectra (see above, Table 1) and in the NMR chemical shifts (see

(5) (a) Nelson, S. M. *Pure Appl. Chem.* **1980**, *52*, 2461. (b) Fenton, D. E. *Pure Appl. Chem.* **1986**, *58*, 1437. (c) Cooper, S. R. In *Crown Compounds: Toward Future Applications*; (Cooper, S. R., Ed.; VCH: Weinheim, 1992; p 112. (d) Menif, R.; Martell, A. E. *J. Chem. Soc., Chem. Commun.* **1989**, 1521.

(6) König, B.; Knieriem, B.; de Meijere, A. *Chem. Ber.* **1993**, *126*, 1643.

Chart 1

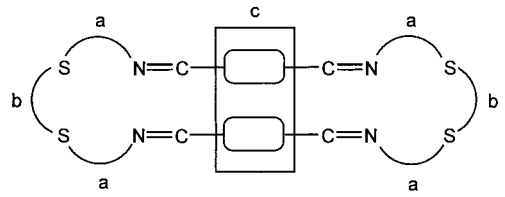

ligand	a	b	c
222			
222-Me			
222-OMe			
phane-222			
Ph2Ph			
232			
242			
323			
333			
meta-222			

Table 1. Electronic Spectra of the Dicopper(I) Compounds

ligand	λ_{max} (nm)			ϵ (dm^3 mol^{-1} cm^{-1})		
222	376	271	203	4070	43 301	58 713
222-Me	380	270	208	8057	54 847	67 105
	321 (sh)					
222-OMe	369	277	204	12 602	15 461	34 005
	224(sh)					
Ph2Ph	380			31 238		
	447 (sh)					
232	368	272	208	4379	42 103	67 684
242	360 (sh)	270	215		60 018	41 905
meta-222	345	230		4183	62 440	
phane-222	309	222		24 222	46 713	
	400 (sh)	283 (sh)				

below), indicating that these effects are electronic in nature. The most prominent effect in the whole series is that of the variation of the chelate ring size (242 vs 232 vs 222) in nitromethane, where the reduction potential shifts from 1370 to 1300 and to 1200 mV (vs NHE) upon reduction of the central chelate ring on each copper center from seven- to six- to five-membered, i.e., the larger cavities stabilize the larger copper(I) ions. In acetonitrile, the potentials of these three compounds vary only marginally (in fact, in acetonitrile the reduction potentials are roughly constant over the whole series of compounds, except for the preorganized ligand phane-222), indicating that, in acetonitrile, the redox active species are structurally very similar. A possible interpretation is that in all these molecules some of the donor groups of the macrocyclic ligands are substituted by acetonitrile molecules, leading to

Table 2. Electrochemical Data of the Double-Helical Dicopper(I) Compounds

	CH_3NO_2		CH_3CN		
ligand	$E_{1/2}$ (mV) vs NHE	ΔE_p (mV)	$E_{1/2}$ (mV) vs NHE	ΔE_p (mV)	scan rate (mV/s)
222[a]	1195	41	1049	45	20
222-Me[b]	1299	93	1192	33	20
222-OMe[b]	1228	78	1057	42	20
Ph2Ph	499	74	−	−	200
232	1300	72	1180	62	10
242[c]	1368	58	1181	50	20
phane-222	−	−	1067	57	20

[a] Without addition of ferrocene. [b] Measurement in CH_3CN without addition of ferrocene. [c] Quasireversible.

unstrained, structurally similar dicopper(I) compounds (see section on dynamics below).

Solid State Structures. The solid-state structures of eight figure-of-eight loop dicopper(I) compounds have been determined by single-crystal X-ray diffraction (the structure of the putative intermediate of the dynamic ring inversion process $([Cu_2(323)(NCCH_3)_2)](ClO_4)_2$) is discussed in a separate section below). Plots of the structures are presented in Figure 1, and crystal data (only those of the structures that have not been reported before) and important structural features are listed in Tables 3 and 4, respectively (full structural data have been deposited to the CCDC (Cambridge Crystallographic Data Centre). For comparison, Figure 1 and Table 4 also include information on the dicopper(I) compounds with meta-substiuted benzene spacer groups (meta-222) and with the paracyclophane-anchored preorganized ligand (phane-222).

All double-helical figure-of-eight loop dicopper(I) compounds that have been characterized so far crystallize in racemic point groups. The elements of chirality for the molecular cations include the helicity based on the coordinated ligand backbone (Δ or Λ), the configuration of the thioether-S donors (*R** or *S**) and the conformation of the chelate rings (λ or δ for the five-membered rings). Due to the conformational flexibility of chelate ring systems and the fact that various chelate ring sizes are involved in the compounds presented here, these will not be discussed in detail. The assignment of the configuration of the coordinated thioether-S donors depends on the ligand structure, i.e., depending on the chelate ring sizes the imine donor substituent or the thioether substituent to a particular coordinated S-donor have the second priority. To generalize the nomenclature, we use the CIP (Cahn−Ingold−Prelog) priorities for the coordinated ligand 222, i.e., $Cu^+ > C_{thioether} > C_{imine} >$ lone pair, to assign the configuration of the coordinated thioether-S donor groups, and the symbols used for this generalized ad-hoc rule are *S*′* or *R*′*. The crystallographically observed configuration in all structures is $\Delta R'^*R'^*R'^*R'^*$ or $\Lambda S'^*S'^*S'^*S'^*$, respectively.

All eight structures are similar, with averaged Cu−S (2.39 ± 0.03 Å) and Cu−N (2.00 ± 0.02 Å) distances in the range expected for copper(I) chromophores, slightly flattened tetrahedral coordination geometries (averaged tetrahedral twist angle $\theta = 72 \pm 1°$), Cu···Cu distances of 7.95 ± 0.18 Å, and a roughly constant distance of the π-stacked benzene spacer groups of 3.54 ± 0.05 Å (the data for the dicopper(I) compounds of meta-222 and phane-222 are excluded for the latter value). The angular geometry about the copper(I) centers of the six structures with identical chelate ring sizes (222, 222-Me, 222-OMe, Ph2Ph, meta-222, phane-222) is roughly identical, with the expected bite angles (S−Cu−S and S−Cu−N) of ca. 90° and a correspondingly enlarged N−Cu−N angle of ca. 145°.

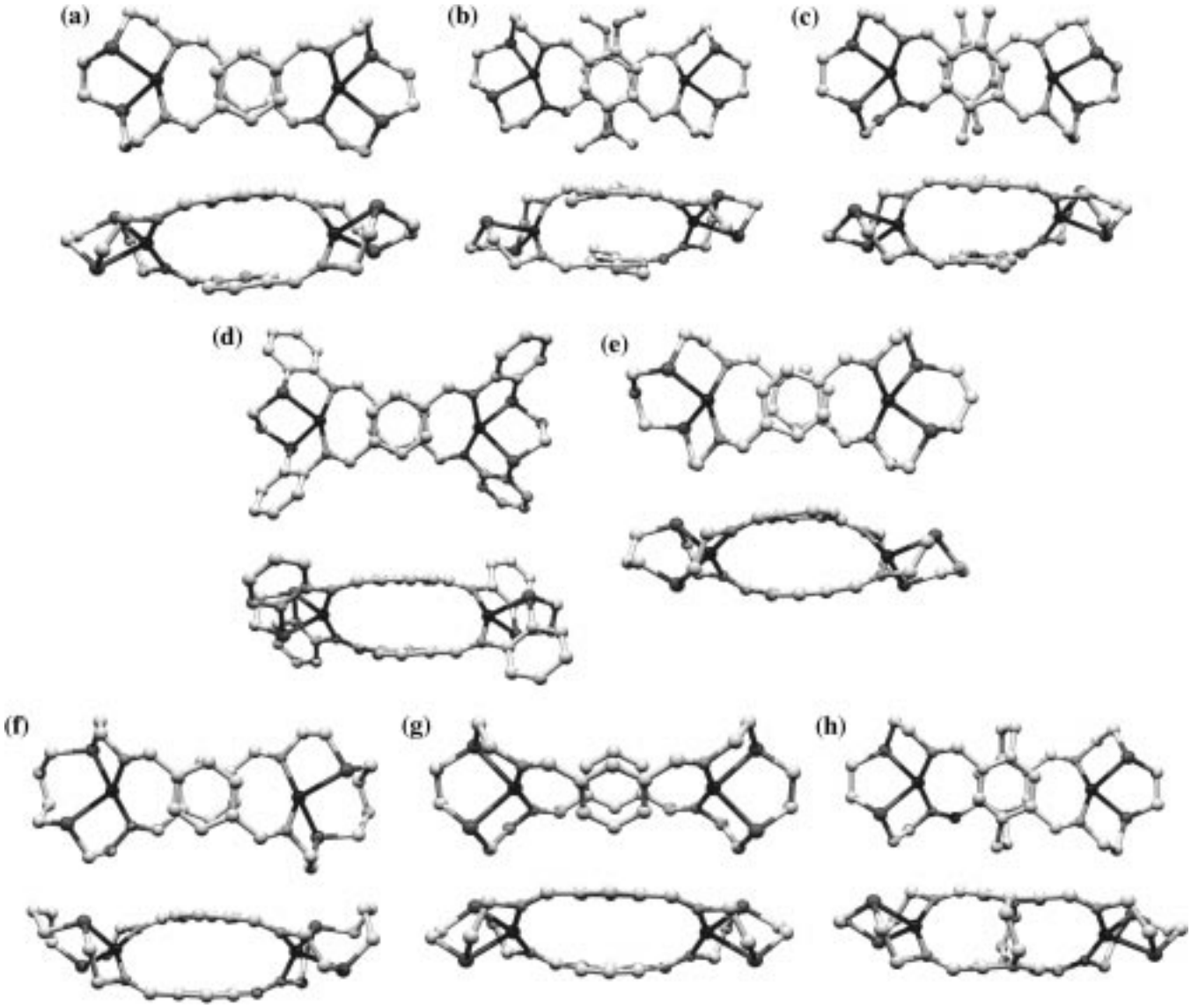

Figure 1. Plots of the experimentally observed structures of the molecular cations of (a) $[Cu_2(222)](ClO_4)_2 \cdot 0.5CH_3CN \cdot 0.5H_2O$, (b) $[Cu_2(222\text{-}OMe)](ClO_4)_2 \cdot 5H_2O$, (c) $[Cu_2(222\text{-}Me)](ClO_4)_2 \cdot 2CH_3CN \cdot H_2O$, (d) $[Cu_2(Ph2Ph)](ClO_4)_2 \cdot 0.5CH_3CN \cdot 0.5H_2O$, (e) $[Cu_2(232)](ClO_4)_2 \cdot H_2O$, (f) $[Cu_2(242)](ClO_4)_2 \cdot 2CHCl_3$, (g) $[Cu_2(meta\text{-}222)](ClO_4)_2 \cdot CH_3CN$, (h) $[Cu_2(phane\text{-}222)](ClO_4)_2 \cdot CH_3CN$.

The increased chelate ring sizes with the ligands 232 and 242 leads to a more relaxed coordination geometry and a small but significant increase in the Cu···Cu distances. Note that relaxation of the geometry refers to the bite angles; the overall tetrahedral twist (slightly flattened tetrahedra) does not change when the S−Cu−S chelate ring sizes vary between five- and seven-membered. The most notable structural differences are observed for the two last entries in Table 4, viz. the compounds with the meta-substituted and with the paracyclophane spacer groups, where, due to the geometry of the spacer groups, the Cu···Cu distances are significantly longer. Note, however, that the copper coordination geometries in these two cases are roughly identical to the other examples with identical chelate ring sizes.

The similarity of the dicopper(I) structures of the self-organized double-stranded helicates, specifically those with identical chelate ring sizes (222, 222-Me, 222-OMe, Ph2Ph), with the geometry of the complex with the preorganized ligand (phane-222) indicates that ligand preorganization is not required to stabilize the figure-of-eight configuration of the dicopper(I) compounds. The variety of structures and lattices involved indicates that intra- rather than intermolecular forces might be responsible for enforcing the double-helical folding. Hence, the folded structures might also be preserved in solution (see below). The stabilization by π-stacking (3−8 kJ mol^{-1})[7] is roughly equalized by the distortion around the imine bond ($C^{imine}-N^{imine}$ ca. 30°, see Table 4; ca. 2 kJ mol^{-1} per bond);[4b,8] hence the folding is believed to be due to the tetrahedral coordination geometry, i.e., unfolding of the helices must probably involve copper-donor bond breaking (see below).

Solution Structures. The question of whether the folded structures of the dicopper(I) compounds are conserved in solution was addressed by ^{1}H NMR spectroscopy in CD_3NO_2, i.e., by the analysis of the coupling patterns of the geminal protons of the methylene groups.[4,9] The simplest example is that involving the ligand with only one set of methylene protons, Ph2Ph, where these appear as a sharp singlet at 2.86 ppm in the metal-free ligand and as a four-line AB pattern in the dicopper(I) compound, with a chemical shift difference of $\Delta\delta$

(7) (a) Petterson, I.; Liljefors, T. *J. Comput. Chem.* **1987**, *8*, 1139. (b) Hobza, P. *J. Phys. Chem.* **1996**, *100*, 1879. (c) Chipot, C. *J. Am. Chem. Soc.* **1996**, *118*, 11217.

(8) Comba, P.; Hambley, T. W.; Hilfenhaus, P.; Richens, D. T. *J. Chem. Soc., Dalton Trans.* **1996**, 553.

Table 3. Crystal Data, Data Collection, and Refinement Parameters[a]

	$[Cu_2(222\text{-}Me)](ClO_4)_2\cdot 2CH_3CN\cdot H_2O$	$[Cu_2(222\text{-}OMe)](ClO_4)_2\cdot 5H_2O$	$[Cu_2(323)(NCCH_3)_2](ClO_4)_2$	$[Cu_2(242)](ClO_4)_2\cdot 2CHCl_3$
emprical formula	$C_{36}H_{50}Cl_2Cu_2N_6O_9S_4$	$C_{32}H_{54}Cl_2Cu_2N_4O_{17}S_4$	$C_{36}H_{50}Cl_2Cu_2N_6O_8S_4$	$C_{34}H_{46}Cl_8Cu_2N_4O_8S_4$
fw	1037.06	1092.88	1020.91	1177.56
color, habit	yellow plates	yellow plates	yellow plates	yellow plates
crystal size/nm			$0.35 \times 0.25 \times 0.05$	$0.40 \times 0.35 \times 0.15$
lattice type	monoclinic	triclinic	monoclinic	triclinic
space group	$C2/c$	$P\bar{1}$	$P2_1/a$	$P\bar{1}$
T/°C	21	21	21	21
cell dimensions				
a/Å	15.039(5)	12.582(2)	9.364(3)	12.832(3)
b/Å	17.332(4)	21.997(4)	23.918(5)	16.292(2)
c/Å	17.850(5)	7.772(2)	10.150(3)	12.460(2)
α/deg		91.45(2)		97.29(1)
β/deg	102.70(2)	93.87(2)	96.53(2)	104.16(1)
γ/deg		78.85(1)		72.17(1)
V/Å^3	4536(2)	2105.4(7)	2258(1)	2400.7(8)
Z	4	2	2	2
D_c/g cm^{-3}	1.518	1.724	1.501	1.629
F(000)	2144	1132	1056	1200
μ	12.96	47.67	85.41	40.68
diffractometer	CAD4	AFC7R	AFC7R	AFC7R
radiation used, λ/Å	Mo Kα, 0.710 69	Cu Kα, 1.5418	Cu Kα, 1.5418	Cu Kα, 1.5418
θ range/deg	$1 < \theta < 25$	$1 < \theta < 60$	$1 < \theta < 60$	$1 < \theta < 60$
no. of measd reflcns	4883	6583	3696	8269
no. of indep reflcns	4432	6251	3463	7145
no. of obsd reflcns	2862	4749	1906	5181
no. of variables	272	554	262	567
R_1, %	0.050	0.062	0.059	0.042
wR_2, %	0.043	0.069	0.074	0.044
weighting factors	$1/\sigma^2(F_o)$	$1/\sigma^2(F_o)$	$1/\sigma^2(F_o)$	$1/\sigma^2(F_o)$

[a] Details in common: graphite-monochromated radiation.

Table 4. Average Bond Lengths (Å) and Angles (deg) of All Dicopper(I) Compounds with the Large Macrocyclic Ligands with $(N_2S_2)_2$ Donor Sets

ligand	222	222-Me	222-OMe	Ph2Ph	232	242	meta-222	phane-222
Cu−S	2.38 (0.02)	2.40 (0.06)	2.40 (0.020	2.34 (0.04)	2.35 (0.03)	2.41 (0.02)	2.43 (0.01)	2.38 (0.02)
Cu−N	2.01 (0.08)	1.98 (0.01)	1.98 (0.02)	2.00 (0.02)	2.02 (0.03)	2.02 (0.02)	1.99 (0.01)	1.96 (0.01)
Cu···Cu	7.83	7.70	7.86	7.77	7.95	8.14	8.15	8.22
$C^{benz}\cdots C^{benz}$	3.43	3.57	3.53	3.42	3.42	3.45	3.26; 3.43	−
benz···benz	3.59	3.55	3.56	3.45	3.49	3.57	3.39	3.09
S−Cu−S	91.0 (0.4)	90.2	90.3 (0.6)	93.1 (0.2)	102.6 (3.4)	103.6 (0.9)	88.2	91.51 (0.2)
S−Cu−N	115.1 (3.7)	114.1 (2.5)	114.8 (5.7)	113.2 (2.2)	116.4 (6.6)	118.8 (8.0)	113.3 (2.4)	117.4 (1.4)
$S-Cu-N^{bite}$	90.8 (1.8)	89.4 (0.6)	89.7 (1.2)	88.0 (0.2)	90.2 (2.0)	88.5 (1.2)	89.7 (0.6)	90.2 (0.6)
N−Cu−N	144.1 (4.2)	147.2	145.4 (0.3)	149.8 (0.4)	138.1 (1.7)	136.1 (0.8)	148.5	141.2 (0.1)
C^{imine}-C^{benz} [a]	31	29	33	23	25	28	27	32
θ[b]	73	72	73	72	73	72	73	71
ϕ[c]	16	14	13	17	19	13	−	−

[a] Torsional angle around the imine bond. [b] Tetrahedral twist angle (S−Cu−S; N−Cu−N planes; tetrahedral: 90°). [c] Torsional angle about the centroids of the benzene spacer groups.

= 1.5 ppm and a geminal coupling of 10.5 Hz.[4a] Here, we present a more thorough analysis of the NMR spectra.

The relevant ^{1}H NMR spectroscopic data (ambient temperature) of the metal-free and coordinated ligands are assembled in Table 5. Some of the spectra of the metal complexes in CD_3CN have not been well resolved at this temperature (see also separate section on dynamics below), but in all cases the peak positions (centers of multiplets) were rather constant within the whole series of ligands and complexes, respectively. Also, where spectra of both the metal-free and coordinated ligands are available (some of the metal-free ligands were not soluble enough for good quality spectra) there is a significant and, with the exception of the aromatic protons, a constant shift of the resonances upon coordination of the ligands to the copper(I) centers. All methylene and imine protons are shifted to lower field upon coordination, as expected due to the shift of electron density to the metal center. The largest chemical shift differences are observed for the imine protons and those of the methylene groups in α position to the thioether donors. The chemical shift differences are generally lower in CD_3CN. This may indicate that the dynamic processes, leading to a loss of resolution (see section on dynamics, below), involve some donor-copper(I) bond breaking in competition with CD_3CN coordination (see also corresponding notes in the section on electrochemistry above). The ^{13}C NMR spectroscopic data (50.3 MHz, ambient temperature, dicopper(I) compounds in CD_3CN; see Table 6) lead to a similar interpretation: (i) the resonances for structurally related carbon atoms are similar in all metal-free ligands; (ii) in the corresponding coordinated ligands, the

(9) (a) Zarges, W.; Hall, J.; Lehn, J.-M.; Bolm, C. *Helv. Chim. Acta* **1991**, *74*, 1843. (b) Ruttimann, S.; Piguet, C.; Bernardinelli, G.; Bocquet, B.; Williams, A. F. *J. Am. Chem. Soc.* **1992**, *114*, 4230. (c) Potts, K. T.; Keshavarz-K, M.; Tham, F. S.; Abruna, H. S.; Arana, C. *Inorg. Chem.* **1993**, *32*, 4436. (d) Fenton, D. E.; Matthews, R. W.; McPartlin, M.; Murphy, B. P.; Scowen, I. J.; Tasker, P. A. *J. Chem. Soc., Chem. Commun.* **1994**, 1391.

Table 5. ^{1}H NMR Data of the Dicopper(I) Compounds and the Metal-Free Ligands at Ambient Temperature[a]

											average	
		222-OMe	222-Me	phane-222	222	232	242	Ph2Ph[b]	323	333[c]	*d*	*e*
dicopper(I) compounds												
imine	CD_3NO_2	8.87[h]	–	8.80[f]	8.65[h]	–	8.65[f]	9.05[f]	–	–	–	–
	CD_3CN	8.78[g]	8.79[f]	8.80[f]	8.60[f]	8.67[f]	8.59[f]	9.05[f]	8.38/8.31[f]	8.48/8.40[f]	8.7 ± 0.1	8.4 ± 0.1
benzene rings	CD_3NO_2	7.30	–	7.68	7.55	–	7.42	8.23	–	–	–	–
	CD_3CN	7.17	7.51	7.68	7.46	7.48	7.37	8.23	7.98/7.87	7.96/7.86[f]	7.5 ± 0.3	7.92 ± 0.06
α-imine	CD_3NO_2	3.98	–	3.85	3.98	–	4.13	–	–	–	–	–
	CD_3CN	3.94	3.89	3.85	3.88	4.07	4.03	–	3.73	3.78	3.9 ± 0.2	3.76 ± 0.03
β-imine	CD_3NO_2	3.05	–	3.06	3.14	–	3.22	–	–	–	–	–
	CD_3CN	2.95	3.07	3.06	3.10	3.16	3.17	–	2.73[i]	2.20/2.78[i]	3.1 ± 0.1	2.75 ± 0.03
α-thioether	CD_3NO_2	3.17	–	3.15	3.13	–	3.13	3.22	–	–	–	–
	CD_3CN	3.10	3.08	3.15	3.10	3.06	3.06	3.22	2.96	2.78	3.1 ± 0.1	2.9 ± 0.1
β-thioether	CD_3NO_2	–	–	–	–	–	2.14	–	–	–	–	–
	CD_3CN	–	–	–	–	2.16	2.07	–	2.00[j]	2.20	–	–
ligands[k]												
imine		–	–	8.25	8.18	8.27	8.27	7.82	8.30	8.30	8.26 ± 0.08	
aromatic		–	–	7.08[l]	7.74	7.74	7.73	7.30	7.75	7.83	7.76 ± 0.07	
α-imine		–	–	–	3.77	3.79	3.78	–	3.73	3.68	3.75 ± 0.07	
β-imine		–	–	–	2.83	2.82	2.79	–	2.57[i]	2.56[i]/1.93	2.7 ± 0.1	
α-thioether		–	–	–	2.74	2.62	2.51	2.68	2.57	2.56	2.6 ± 0.15	
β-thioether		–	–	–	–	1.85	1.75	–	1.95[j]	1.93	–	

[a] In ppm; centers of the multiplets. [b] Not included in the average (ring current effects of the benzene groups). [c] Only NMR data are reported for this compound. [d] Helical form (all ligands except 333 and 323; measured in acetonitrile). [e] Nonhelical form (ligands 323 and 333; measured in acetonitrile). [f] 200 MHz. [g] 300 MHz. [h] 500 MHz. [i] *γ*-Imine methylene protons. [j] *β*-Imine methylene protons. [k] In $CDCl_3$ at 200 MHz. [l] Not included in average.

Table 6. ^{13}C NMR Data (50.3 MHz) of the Dicopper(I) Compounds (Acetonitrile) and of the Metal-Free Ligands (Chloroform)[a]

										average	
	222-OMe[b]	222-Me	phane-222	222[b]	232	242	Ph2Ph[c]	323	333	*d*	*e*
dicopper(I) compounds											
imine	163.9	164.7	164.1	166.3	166.6	166.9	165.6	164.5	163.7	165.3 ± 1.6	164.1 ± 0.4
aromatic (C-H)	110.4[c]	129.0	129.3	129.1	129.1	128.2	128.1	129.7	130.6	128.9 ± 0.7	130.2 ± 0.5
aromatic (C-imine)	127.9[c]	136.9	138.2	138.4	138.1	137.8	135.4	138.6	138.9	137.9 ± 1.0	138.8 ± 0.2
α-imine	59.7	58.9	59.2	59.2	61.0	62.4	*f*	62.7	62.1	60.1 ± 2.3	62.4 ± 0.3
β-imine	34.5	34.6	34.9	34.4	36.2	38.4	*f*	35.0[g]	33.0[g]/33.6	35.5 ± 2.9	34.0 ± 1.0
α-thioether	33.5	33.1	34.2	33.2	32.9	35.9	38.3	33.4	30.2	33.8 ± 2.1	31.8 ± 1.6
β-thioether	56.9[h]	18.7[h]	33.2[i]	–	26.1	29.1	–	30.4[j]	26.7	–	–
ligands											
imine	–	–	–	161.4	161.6	161.5	159.5	160.9	160.2	161.2 ± 1.0	
aromatic (C-H)	–	–	–	128.5	128.4	128.4	129.2	128.3	128.5	128.4 ± 0.2	
aromatic (C-imine)	–	–	–	138.0	137.9	138.0	135.8	138.0	137.5	137.9 ± 0.4	
α-imine	–	–	–	62.7	61.9	61.7	*k*	60.0	60.0	61.3 ± 1.4	
β-imine	–	–	–	33.3	32.8	32.8	*k*	29.8[g]	30.3[g]/30.8	32.0 ± 2.2	
α-thioether	–	–	–	33.1	31.2	32.1	33.5	30.5	29.7	31.8 ± 2.1	
β-thioether	–	–	–	–	29.4	28.7	–	32.1[j]	29.2	–	

[a] In ppm. [b] 75.5 MHz. [c] Not included in the average. [d] Helical form (all ligands except 333 and 323; measured in acetonitrile). [e] Nonhelical form (ligands 323 and 333; measured in acetonitrile). [f] Benzene groups in the chelate rings (C_{imine}, 152.4; *ortho*-C_{imine}, 123.3; *meta*-C_{imine}, 131.5; $C_{thioether}$, 141.0; *ortho*-$C_{thioether}$, 132.5; *meta*-$C_{thioether}$, 131.5). [g] *γ*-Imine methylene group. [h] Methyl carbon of the methyl and methoxy groups. [i] Methylene carbon of the ethylene bridges in the paracyclophane group. [j] *β*-Imine methylene group. [k] Benzene groups in the chelate rings (C_{imine}, 149.8; *ortho*-C_{imine}, 114.4; *meta*-C_{imine}, 129.8; $C_{thioether}$, 137.9; *ortho*-$C_{thioether}$, 116.4; *meta*-$C_{thioether}$, 129.8).

resonances are similar within the whole series but generally shifted to lower field with respect to the metal-free ligand molecules.

There are two types of aromatic protons of the unsubstituted *p*-xylylene spacer groups, labeled with X and Y in Figure 2 (oriented toward the periphery of the dinuclear compounds or toward the coordination centers, respectively). Upon double-helical folding, all benzene protons of the spacer groups must experience the influence of the ring current of the *π*-stacked aromatic ring. In the preorganized ligand phane-222 the interaction due to *π*-stacking is already present in the metal-free ligand (δ_{ar} = 7.08 ppm vs 7.76 ± 0.07 ppm for all other ligands). Hence, taking the differences due to substituents, strain in the paracyclophane fragment and differences in the benzene···benzene distance into account, the assumed effect due to the direct dipole−dipole interaction from *π*-stacking is a shift of ca. 0.3−0.5 ppm to higher field. Upon coordination to copper(I) the aromatic protons of phane-222 are shifted by 0.6 ppm toward lower field. The dicopper(I) complex of phane-222 has only aromatic protons of the type Y (see left enantiomer Figure 2). Thus, a low-field shift of 0.6 ppm may be assigned to direct dipole-dipole interaction with the copper(I) center. None of the double-helical dicopper(I) complexes with two types of aromatic protons has resolved signals for protons X and Y at ambient temperature, suggesting a dynamic process in solution. Thus, in these examples, the low field shift due to the interaction with the copper(I) centers is averaged over two aromatic protons (ca. 0.3 ppm each) and partially canceled by a high field shift of 0.3−0.5 ppm due to *π*-stacking.

For three of the double-helical dicopper(I) species (ligands 222, 242, 222-OMe) the solution structure has been confirmed by high-resolution ^{1}H NMR spectra in CD_3NO_2. That of $[Cu_2(222)]^{2+}$ is shown in Figure 3. The assignment of the signals

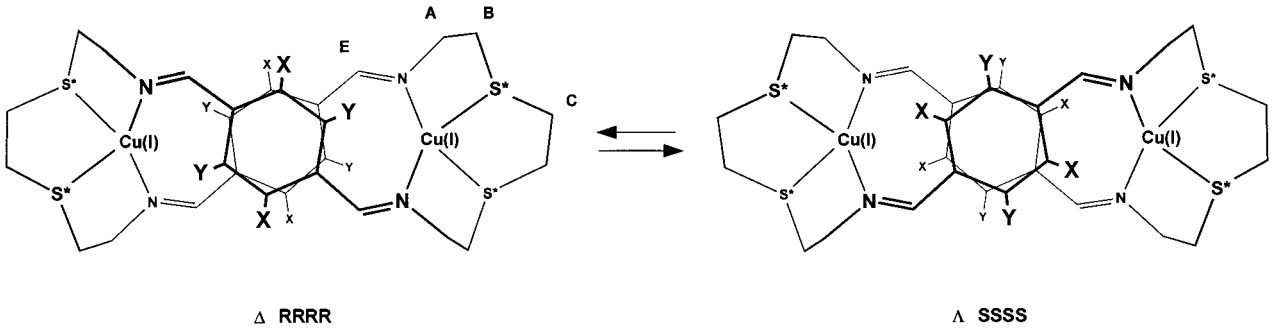

Figure 2. Two enantiomeric forms of the double-helical dicopper(I) compounds and the labeling of the protons. Shown is the dicopper(I) cation of 222. For 242 the central methylene groups of the butyl fragment are labeled with D.

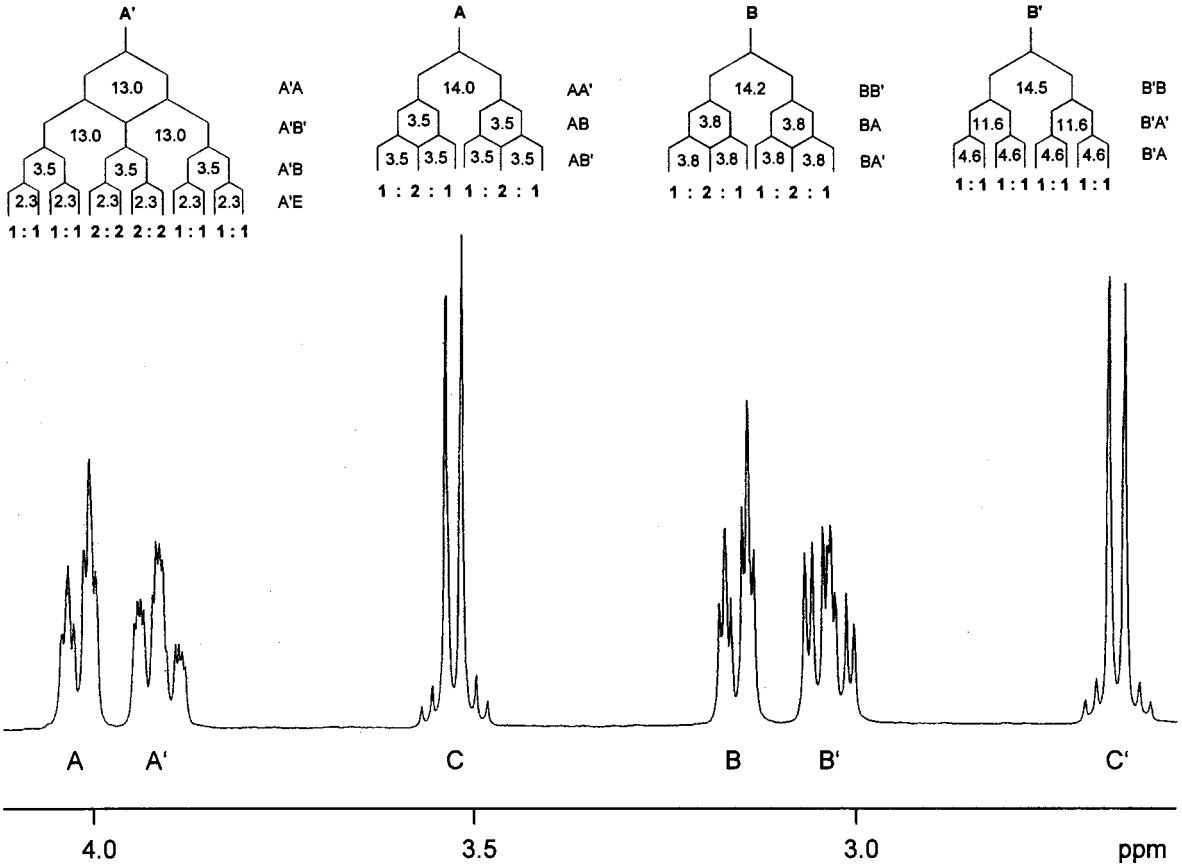

Figure 3. 500 MHz ^{1}H NMR spectrum of $[Cu_2(222)]^{2+}$, aliphatic region (singlets for imine and aromatic protons at δ 8.65 ppm and 7.55 ppm).

is based on two-dimensional homonuclear (H,H)-correlated magnetic resonance spectra (analysis of the cross-peaks in the ^{1}H−^{1}H COSY 90−45° spectra), and the analysis of the spin systems is given in Figure 3. The coupling patterns and the coupling constants are indicative of intact chelate rings, and, together with the chemical shifts (see analysis above), they support the assignment of a double-helical structure. Note, that the interpretation of the high-resolution ^{1}H NMR spectra is based on 1st order analysis; the names of the sites A, A′,B, B′, C, and C′ (see Figure 2) do not imply any structural or magnetic similarity.

The chelate ring torsion angles have been analyzed with Karplus relations, involving the ^3J coupling constants (see Figure 3).[10] In Table 7, the calculated torsion angles are compared to those from the solid-state structures. Also included in Table 7 are the calculated torsion angles based on the $^4J(H_A-H_E)$ long-range coupling. The agreement between observed torsion angles (solid-state structures) and those calculated from the high-resolution ^{1}H NMR spectra is acceptable, i.e., the conformations in the solid and in solution are similar. Note that, generally, an inversion of an unsubstituted chelate ring does not influence the coupling pattern, i.e., the fact that the conformations in the solid and in solution are similar does not indicate conformational rigidity. The situation is slightly complicated for the chelate rings adjacent to the imine groups. The long-range coupling $^4J(H_A-H_E)$ across the imine double bond is angle dependent, with a maximum coupling at a torsion angle of 90°. From Table 7 it emerges that the inversion of the imine-N/thioether-S chelate ring leads to a change in the orientation of the imine proton with respect to the α-methylene protons in the chelate ring. However, in each of the two conformations of the five-membered chelate rings, one of the two methylene protons is coupled to the imine proton. We assume that the observed coupling pattern is the result of an only partly resolved pattern,

(10) Friebolin, H. *Ein- und zweidimensionale NMR-Spektroskopie*, 2nd ed.; VCH: Weinheim, 1992; p 88.

Table 7. Analysis of the Conformations of the Dicopper(I) Compounds of the Two Ligands 222 and 242

	solution (Karplus relation[a])		solid (X-ray) torsional angle (deg)			
pair of protons	torsional angle (deg)	^3J coupling constant (Hz)				
242						
AB	55−85	2	56	63	the two chromophores have nearly identical conformations of the chelate rings	
AB′	145−180	14	175	177		
A′B′	45−70	4	55	55		
A′B′	85−95	0	63	64		
CD	135−170	10	177	154		
C′D′	30−60	5	30	55		
CD′	85−95	0	64	88		
C′D	85−95	0	88	63		
222						
AB	30−60	4	73	73	80	69
AB′	30−60	4	46	48	37	52
A′B	30−60	4	44	43	34	53
A′B′	>150	13	162	165	152	174

torsion between imine protons E and A	solid (X-ray; λ, deg)		inverted chelate ring (δ, deg)	
222				
EA	24	11	54	44
EA′	93	112	68	72
242				
EA	21	11	37	47
EA′	98	131	82	72

[a] Reference 10.

due to a fast equilibration on the NMR time scale, of the two conformations of the five-membered rings (λ/δ). Thus, the agreement between solid state and solution torsion angles supports configurational rigidity, i.e., the overall structures in solution are similar to those observed in the crystals, and this emerges not only from the analysis of the torsion angles but also from the observed chemical shifts and coupling patterns.

Dynamics. Various dynamic processes are possible in the double-helical dicopper(I) compounds. (i) Chelate ring inversion. Due to the variety of chelate ring sizes considered here, these processes are not analyzed explicitely. Also, these are generally fast with activation energies of the order of 20−50 kJ mol^{-1}, viz. they are faster than the time scale of the NMR experiments described here.[11] (ii) Inversion of the thioether-S donors with retention of the helicity. These are equilibria involving various diastereoisomers ($\Lambda S'^*S'^*S'^*S'^*$; $\Lambda R'^*S'^*S'^*S'^*$; $\Lambda R'^*R'^*S'^*S'^*$; $\Lambda R'^*S'^*R'^*S'^*$; $\Lambda R'^*S'^*S'^*R'^*$; $\Lambda R'^*R'^*R'^*S'^*$; $\Lambda R'^*R'^*R'^*R'^*$; and the corresponding forms with Δ helicity since racemic compounds are used here) with different stabilities and abundances. (iii) Inversion of the helicity with retention of the configuration at the thioether-S donors. This is an equilibrium between the two diastereomeric forms $\Lambda S'^*S'^*S'^*S'^*$ and $\Delta S'^*S'^*S'^*S'^*$ (and the corresponding enantiomers with all thioether-S donors in R'^* configurations since racemic compounds are discussed here). (iv) Racemization, i.e., concerted inversion of the helix and all thioether-S donor groups.

Inversion of the thioether-S donors involves Cu−S bond breaking, and, therefore, it is expected that this process has an activation barrier that is higher than that of the helix inversion process. Hence, the only example, where inversion of thioether-S donors with retention of the helix configuration may be observed is the dicopper(I) compound of phane-222, where the helix is fixed by the paracyclophane anchor group. The fact that no inversion processes at the thioether-S donors of $[Cu_2(\text{phane-222})]^{2+}$ were observed (see below) indicates that either the crystallographically observed pair of enantiomers $\Lambda S'^*S'^*S'^*S'^*/\Delta R'^*R'^*R'^*R'^*$ is the only stable diastereomer and/or the Cu−S bond breaking involves a transition state where the stacking of the benzene spacer groups is distorted or removed.

Inversion of the Helix. The ^{1}H NMR spectroscopic data indicate that the solid state structure is conserved in nitromethane solution (see above). The fact that only one instead of at least two signals for the aromatic protons are observed (protons X and Y in Figure 2 above; in all ligands except phane-222, 222-Me, 222-OMe, where only one aromatic proton is present) indicates that there is a fast process on the NMR time scale that interconverts the two protons. Full conservation of the chromophore, i.e., no Cu−S and/or Cu−N bond breaking, indicates that this process is a dynamic equilibrium between the two diastereomers $\Lambda S'^*S'^*S'^*S'^*$ and $\Delta S'^*S'^*S'^*S'^*$ (and the corresponding enantiomers since racemic compounds are studied; this is an epimerization process). Thus, at low temperature two pairs of signals with different intensities should be observed, each consisting of two doublets (coupled protons X and Y), i.e., 8 signals altogether. Dicopper(I) compounds with only one type of aromatic protons (substituted *p*-xylylene spacer groups) should lead to two singlets, one for each diastereomer.

Variable-temperature ^{1}H NMR studies of the dicopper(I) compounds of all ligands indicate that, with the exception of those that have only one type of aromatic protons (phane-222, 222-Me, 222-OMe), with decreasing temperature there is a line broadening of the signal for the aromatic protons (ca. 7.5 ppm). At the lowest temperature accessible in the solvents used (CD_3CN, CD_3NO_2, 230 K) the signal splits into two relatively broad singlets in the cases of 232, 242, and Ph2Ph (for the ligands 323 and 333 the dicopper(I) compounds are assumed not to have a stable helical configuration). The only spectrum with reasonably well resolved aromatic signals is that of $[Cu_2(242)]^{2+}$. For this, high-resolution (500 MHz) variable-temperature spectra were recorded, and these are shown in Figure 4 and discussed in detail.

The qualitative observations of line broadening and the measured coalescence temperatures (Table 8, last column) are independent of the solvent used. This supports the interpretation that the exchange process does not involve any bond breaking (see section on racemization, below). The chemical shift of the two resolved signals for $[Cu_2(242)]^{2+}$ (7.2 and 7.6 ppm) are similar to those observed for the preorganized metal-free ligand (phane-222) and its dinuclear complex ($[Cu_2(\text{phane-222})]^{2+}$), respectively (see Table 5 above), i.e., the higher field signal may be assigned to proton X and the lower field signal to proton Y of the left enantiomer in Figure 2 above. Thus, we interpret the process leading to coalescence of these two protons as a fast reversible torsion around the centroids of the two benzene spacer groups (in contrast to the racemization process shown in Figure 2, the helix inversion discussed here is an epimerization with retention of the configuration of the thioether-S donors).

The helix inversion with full conservation of the chromophore must also lead to a torsion around the $C^{benzene}-C^{imine}$ bond, and model studies indicate a drastic change in the orientation of the imine proton (see also section on solution structures above). The observation of a specific pattern of torsion angles in the

(11) Hambley, T. W. *J. Comput. Chem.* **1987**, *8*, 651.

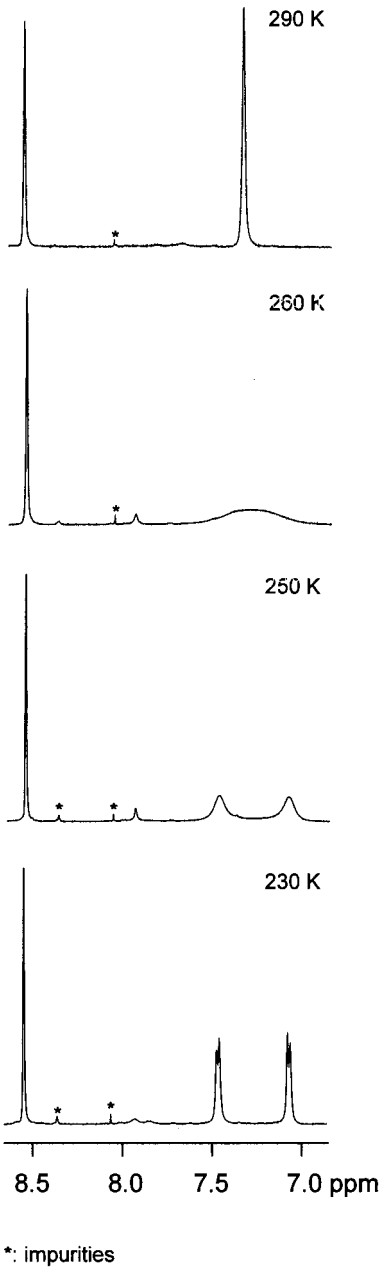

Figure 4. Temperature-dependent 500 MHz ^{1}H NMR spectra of $[Cu_2(242)]^{2+}$ (230, 250, 260, 290 K; CH_3NO_2; low-field region).

ligand backbone (see discussion of the data of Table 7) indicates that the helix inversion must be accompanied by a fast relaxation of various torsion angles (chelate ring inversion). Due to the low activation energies for chelate ring inversion (ca. 20−50 [12] vs ca. >50 kJ mol^{-1} emerging from the coalescence temperature for the helix inversion, Table 8), we assume a concerted mechanism for the helix-inversion/chelate-ring-inversion process. This is supported by the observed rate for the helix inversion that increases in the series Ph2Ph < 242 < 232 < 222 (Table 8), i.e., the inversion of five-membered chelate rings generally has lower inversion barriers than that of larger rings,[11,13] and the rigidity of the phenyl substituted rings is also in agreement with the lower helix interconversion rates.

The spectra shown in Figure 4 are not well enough resolved to detect the resonances of the aromatic protons for the less abundant diastereomer with the inverted helix. However, when the temperature is lowered, a new small singlet appears at 7.95 ppm. This is attributed to the resonance of the imine proton of the $\Delta S'^*S'^*S'^*S'^*/\Lambda R'^*R'^*R'^*R'^*$ conformer. The significant high-field shift is in agreement with the expectations (see solution structure above). Integration of the two signals for the imine protons at 230 K indicates that the isomer distribution is approximately 9:1, i.e., there is an energy difference between the two diastereomers of approximately 5.5 kJ mol^{-1}. It is of interest to remember that only the more stable configuration ($\Lambda S'^*S'^*S'^*S'^*/\Delta R'^*R'^*R'^*R'^*$) has been observed in all crystal structures analyzed so far. No resonances for the diastereomer with the inverted helix have been observed in the region of the aliphatic protons. We assume that the chemical shift differences are minimal (the environment of the protons is primarily determined by the coordination geometry), and the low concentration of the less stable isomer precludes the detection of these extra signal in the area of the multiplets for the methylene protons.

Racemization. The second dynamic process observed for the double-helical dicopper(I) compounds is, in contrast to the helix inversion, solvent dependent. At high temperatures in CD_3CN the ^{1}H NMR spectra of all dicopper(I) compounds with the exception of that of $[Cu_2(phane\text{-}222)]^{2+}$ are, in terms of the coupling patterns, similar to those of the corresponding metal-free ligands. The chemical shifts of all protons are still shifted to lower field (except for the aromatic protons), due to coordination to the metal centers (see Table 5), but there is no difference between axial and equatorial protons, i.e., the ABCD spin systems of the five-membered chelate rings (and the corresponding spin systems of the larger rings; see Figure 3), due to vicinal, geminal, and long-range coupling change to simple AB systems (exclusively vicinal coupling). The UV−vis and electrochemical data together with the fact that the resonances are shifted to lower field with respect to the metal-free ligand molecules indicate that the ligands are, on average, still coordinated to copper(I). The significant solvent dependent differences in all these properties suggest, however, that in average the copper(I)−imine and/or the copper(I)−thioether bonds are weakend (or part or all of them are broken at an intermediate state) in acetonitrile (see comments in various sections above, specifically on electrochemistry and NMR chemical shifts). Acetonitrile is known to bind strongly to copper(I). Thus, the solvent dependence suggests that acetonitrile competes with the ligand donor groups and therefore leads, through fast ligand exchange, to a dynamic process involving racemization, i.e., a concerted helix inversion and inversion of all thioether-S donors ($\Lambda S'^*S'^*S'^*S'^* \leftrightarrow \Delta R'^*R'^*R'^*R'^*$). A typical sequence of ^{1}H NMR spectra is shown in Figure 5, and the coalescence temperatures for the double-helical dicopper(I) compounds are given in Table 8.

From the fact that the reversible coordination of acetonitrile is responsible for the inversion of the thioether-S centers it follows that equilibration at high temperature should produce all possible diastereomers (four thioether-S donors (R'^* or S'^* each) and the helix (Δ or Λ), i.e., seven nondegenerate structures). The fact that, when "equilibrated" solutions are measured at low temperature, only one isomer, i.e., that observed in all crystal structures ($\Lambda S'^*S'^*S'^*S'^*/\Delta R'^*R'^*R'^*R'^*$) is observed, indicates again that this is by far the most stable structure. The fact that for $[Cu_2(phane\text{-}222)]^{2+}$ no dynamic

(12) Hesse, M.; Meier, H.; Zeeh, B. *Spektroskopische Methoden in der Organischen Chemie*, 4th ed.; Georg Thieme Verlag: Stuttgart, 1991; p 96.

(13) (a) Niketic, S.; Rasmussen, K.; Woldbye, F.; Lifson, S. *Acta Chem. Scand.* **1976**, *A30*, 485. (b) Niketic, S.; Rasmussen, K. *Acta Chem. Scand.* **1981**, *A35*, 213.

Table 8. Temperature Dependent ^{1}H NMR Spectra (200 MHz) of the Dicopper(I) Complexes[a]

ligands	no. of ring atoms	double-helical structure	coalescence temperature (K) imine−thioether−chelate (in CD_3CN)	coalescence temperature (K) thioether−thioether−chelate (in CD_3CN)	coalescence temperature (K) aromatic spacer groups (in CD_3CN and CD_3NO_2)
222	32	yes	270	300	<230
222-OMe	32	yes	320	340	−
222-Me	32	yes	330	350	−
Phane-222	32	yes	no coalescence	no coalescence	−
Ph2Ph[b]	32	yes	−	290	260
232	36	yes	280	290	230
242	36	yes	280	290	245
323	36	no	≪230	≪230	−
333	38	no	≪230	≪230	−

[a] Accuracy of T: ±5 K. [b] In CD_3CN/CD_3NO_2 (1:1, see text).

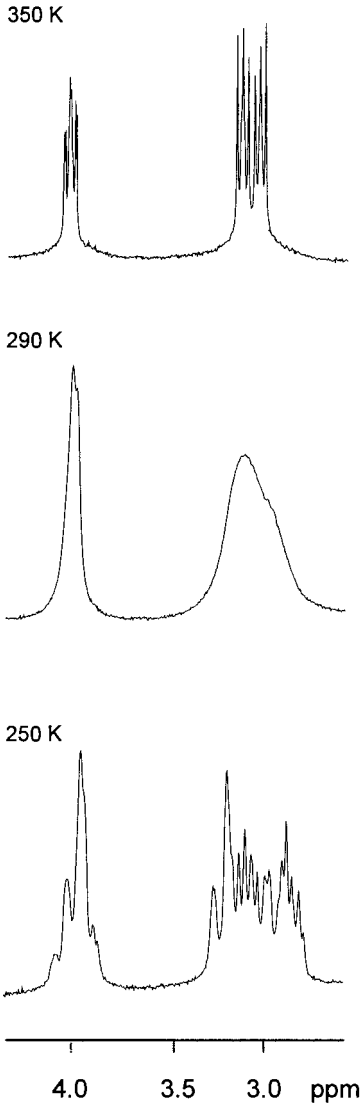

Figure 5. Temperature-dependent 200 MHz ^{1}H NMR spectra of $[Cu_2(232)]^{2+}$ (250, 290, 350 K; CH_3CN; high-field region).

process is observed in CD_3CN at elevated temperatures might be used to support this interpretation. However, the necessary supposition for the equilibration of the configuration of the thioether-S donors is ligand exchange with acetonitrile, and this was observed indirectly in electrochemical experiments (CH_3CN vs CH_3NO_2; Table 4) and ^{1}H NMR chemical shifts (CD_3CN vs CD_3NO_2; Table 5) of the dicopper(I) compounds. The fact that the spectroscopic behavior of $[Cu_2(\text{phane-222})]^{2+}$ is solvent independent suggests that in this case there is no ligand exchange with acetonitrile. We interpret this observation with a concerted helix inversion/acetonitrile coordination/thioether-S inversion sequence for all double-helical dicopper(I) compounds, i.e., the ligand exchange reaction with acetonitrile is activated along the $\Lambda S'^*S'^*S'^*S'^* \leftrightarrow \Delta S'^*S'^*S'^*S'^*$ reaction coordinate, and this is not possible for the paracyclophane anchored species. Model studies support this interpretation, i.e., the copper(I) centers are well protected by the ligand backbone in the more stable $\Lambda S'^*S'^*S'^*S'^*$ configuration, whereas along the helix inversion reaction and at the inverted helix ($\Delta S'^*S'^*S'^*S'^*$) the metal centers are more accessible for ligand substitution.

This interpretation is further supported by the fact that the racemization rate is significantly smaller (increase of the coalescence temperature by ca. 50 K) for the two ligands with substituted benzene spacer groups (222-Me and 222-OMe), where the helix inversion is desactivated (Table 8). There is no experimental evidence for a helix inversion (with retention of the thioether-S configuration) for these two substituted compounds, and for steric reasons this seems to be an unfavorable process (formal exchange of the Me and OMe xylylene substituents between positions X and Y, see Figure 2). Therefore, we suggest that the activation of the ligand exchange reaction occurs along rather than after the helix inversion. Hence, the observed racemization of the two *p*-xylylene substituted compounds must occur at an (at least partially) ring-open intermediate, and this mechanism is shown in Figure 6. Note that, for steric reasons, in the case of the two compounds with substituted *p*-xylylene spacer groups (222-Me and 222-OMe) the inverted structures ($\Lambda S'^*S'^*S'^*S'^*$ vs $\Delta R'^*R'^*R'^*R'^*$) both have the xylylene substituents pointing to the periphery of the double helicates. Thus, at an intermediate state, there must be free rotation of the xylylene groups, and this is further support for a mechanism involving bond breaking to the imines for the racemization process.

Crystal Structure of a Partly Unfolded Intermediate. The fact that copper-donor bond breaking is assisted by the reversible coordination of acetonitrile is further supported by an X-ray crystal structure analysis of a putative intermediate. The dicopper(I) complex of 323 crystallizes with two imine donors (one at each coordination site) substituted by acetonitrile ($[Cu_2(323)(NCCH_3)_2]^{2+}$). A structural diagram of the complex cation is shown in Figure 7, and the crystallographic data and relevant geometric parameters are given in Tables 3 and 9, respectively. The fact that acetonitrile does not only substitute the imine but also to the thioether-S donor groups is not only a requirement for the inversion of the thioether-S donors, it also follows from the chemical shift differences of the methylene protons in the thioether chelate rings in dependence of the solvent (Table 5)

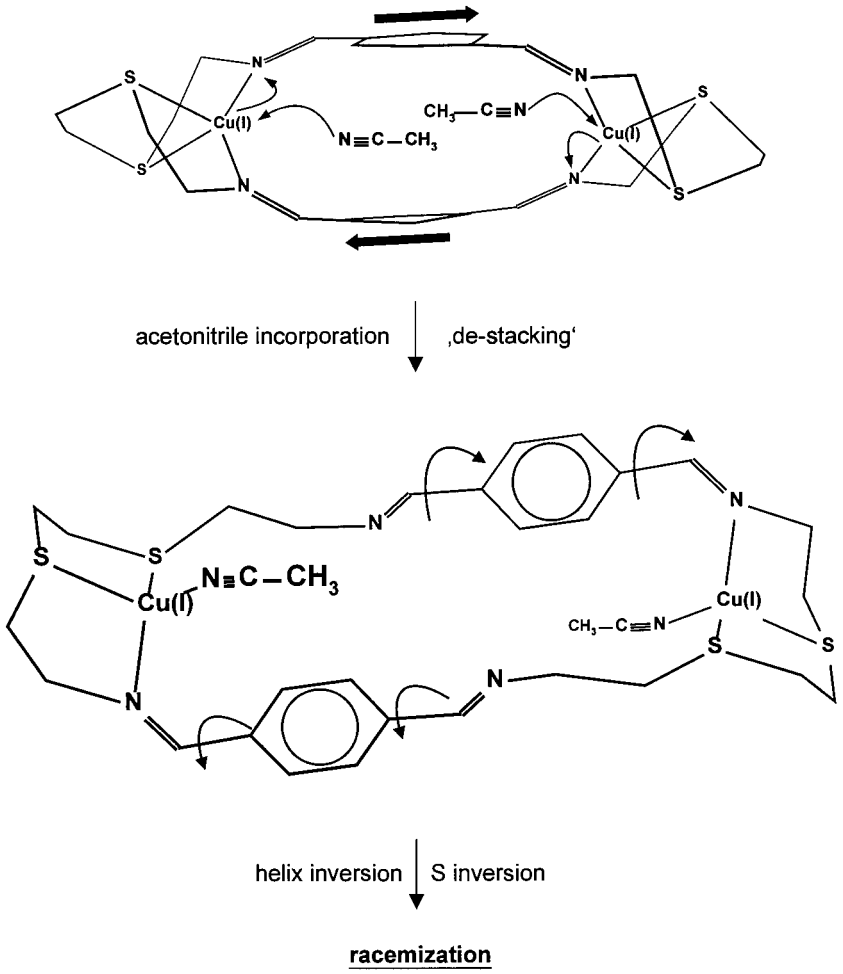

Figure 6. Mechanism of the racemization of the double-helical figure-of-eight loop dicopper(I) compounds.

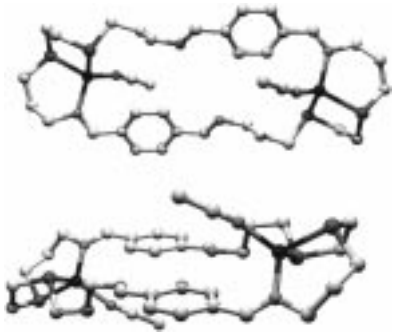

Figure 7. Plot of the experimentally observed structure of the cation of $[Cu_2(323)(NCCH_3)_2](ClO_4)_2$.

Table 9. Average Bond Lengths (Å) and Angles (deg) in $[Cu_2(323)(NCCH_3)_2](ClO_4)_2$

Cu−S	2.32 (0.01)
Cu−N	2.01 (0.01)
Cu···Cu	12.02
$C^{benz}\cdots C^{benz}$	5.15
benz···benz	7.88
S−Cu−S	93.5
S−Cu−N	114.7
$S-Cu-N^{bite}$	107.3
N−Cu−N	108.5[a]
$C^{imine}-C^{benz}$	29/10[b]

[a] One nitrogen atom is from the coordinated acetonitrile. [b] The torsional angle involving a coordinated imine is smaller.

and from the coalescence of the corresponding methylene signals (Table 8). The fact that the exchange process involving the thioether chelate rings is generally significantly slower than that of the thioether−imine chelates indicates that, as expected for steric reasons, the exchange at the imine donors is kinetically favored. The fact that the crystallized compound with one acetonitrile coordinated to each of the copper(I) centers fits nicely in this picture.

Macrocycles with propylene bridges between the imine-N and the thioether-S donors do not lead to stable double-helical dicopper(I) compounds. There are at least two possible interpretations for this observation. (i) From the discussion of the structural features it emerges that the (distorted) tetrahedral coordination to the copper(I) centers (see Figure 1 and Table 4) is the reason for the double-helical folding. The increased flexibility in the imine-N/thioether-S chelate rings may lead to the preference for other structural possibilities, i.e., rigid chelate rings adjacent to the benzene spacer groups are a requirement for the double-helical folding. (ii) The observed instability of the dicopper(I) compounds with 323 and 333 might also further support the mechanism that involves the activation of the racemization reaction (i.e. the decay of the double-helical structures) by substitution of the $Cu-N^{imine}$ bond with solvent donor groups. Due to the flexibility of the six-membered chelate rings the less powerful donor nitromethane might be an effective enough donor to promote this reaction path. Further support for this interpretation emerges from the relatively large difference in the coalescence temperature of the aromatic protons between 222 and Ph2Ph, i.e., the flexibility of the five-membered chelate rings is further suppressed by the benzene substitution.

Conclusions

High-field ^{1}H NMR spectroscopy indicates that the structures of the dicopper(I) compounds of the 32- to 36-membered macrocyclic $(N_2S_2)_2$ ligands are similar to the solid-state structures, i.e., figure-of-eight loop double-helical. The structural similarity between the dicopper(I) compounds of all macrocyclic ligands, including that with the *m*-xylylene spacer group, but especially that with identical chelate rings, i.e., 222, with the preorganized, paracyclophane-based ligand, indicates that ligand preorganization is not a prerequisit for the double-helical figure-of-eight structures. The fact that the self-organized double helices are structurally very similar to that of the dicopper(I) compound of the paracyclophane based ligand also suggests that steric rather than electronic reasons might be responsible for the observed structural features in the solid state and in solution. This also follows from a qualitative analysis of the energies involved in the π stacking of the benzene spacer groups and the distortion of the imine donor functions.

Two dynamic processes have been identified in solution; the first is a solvent-independent inversion of the helix with full conservation of the configuration of the thioether-S donors, i.e., an epimerization that involves two diastereomeric forms of the dicopper(I) compounds in approximately a 9:1 ratio. The second process, the racemization involving five stereogenic elements (the helicity of the macrocyclic ligand and the four thioether-S donors), has only been observed in the coordinating solvent acetonitrile. The fact that copper(I) to donor bond breaking is an important feature of the racemization process is supported by the observed solvent dependent ^{1}H NMR chemical shifts, the UV−vis and electrochemical data, the variable-temperature ^{1}H NMR experiments and a crystal structure analysis of a putative intermediate. The whole set of experimental data, involving structural, spectroscopic and kinetic results of the entire series of ligands and complexes in the solid, in acetonitrile and in nitromethane solution suggest that racemization of the double-helical dicopper(I) compounds involves (i) activation by a torsion around the centroids of the xylylene spacer groups, (ii) substitution of copper(I)−macrocyclic donor bonds by acetonitrile, (iii) free rotation of the xylylenyl spacer groups around the $C^{imine}-C^{benzene}$ bonds, and (iv) inversion of the coordinated thioether-S donors by a fast reversible substitution with acetonitrile.

Experimental Section

General. The diaminodithiaalkanes were prepared as described previously.[4,14] The benzenedialdehydes are commercially available or synthesized by literature procedures. NMR spectra were obtained with a Bruker AS 200 instrument at 200 (300) and 50.32 (75.5) MHz for ^{1}H and ^{13}C NMR, respectively. High-resolution ^{1}H NMR spectra (500 MHz) were recorded with a Bruker Spectrospin DRX 500 instrument. Infrared spectra (KBr pellets) were measured with a Perkin-Elmer 16PC FT-IR instrument. UV−vis spectra were obtained with a Cary 1E or a Cary 2300 instrument. Electrochemical measurements of 5.0 mM solutions of the complexes in $MeNO_2$ or MeCN, containing 0.1 M tetrabutylammonium perchlorate as electrolyte and ferrocene as internal standard (+0.56 V vs NHE), were made with a BAS 100B instrument with a glassy carbon working electrode, a Pt auxiliary electrode and a Ag/AgCl reference electrode. Mass spectra were recorded with a Finnigan 8400 mass spectrometer. Elemental analyses were obtained from the microanalytical laboratory of the chemical institutes of the University of Heidelberg.

Syntheses. All macrocyclic ligands and their dicopper(I) compounds were prepared essentially in the same way; those of 222,[4b] Ph2Ph,[4a] *meta*-222[4b] and 232[4a] have been reported previously. Solutions of the macrocyclic ligands 222-Me and 222-OMe were coordinated to copper(I) without isolation. The synthesis of 222-phane will be given in a separate section below.

To a vigorously stirred solution of the dithiadiamine (31.5 mmol) in acetonitrile (800 mL) was slowly added (over 24 h) an acetonitrile solution (500 mL) of the dialdehyde (31.5 mmol). The isolated yellowish/white solids of the product were recrystallized twice from CH_3CN/CH_2Cl_2 (1:1).

242. Yield: 6.7 g (10.9 mmol; 69.5%). MS (FAB$^+$, NOBA), *m*/*z*: 612 (6) [M$^+$]. ^{1}H NMR (200 MHz, $CDCl_3$): δ 8.27 (s, 4H, NCH), 7.73 (s, 8H, Ar-H), 3.78 (t, 8H, NCH_2), 2.90 (t, 8H, NCH_2CH_2), 2.51 (t, 8H, SCH_2), 1.60−1.91 (m, 8H, SCH_2CH_2). ^{13}C NMR (50.3 MHz, $CDCl_3$): δ 161.5 (NCH), 138.0 (Ar-*C*-CHN), 128.4 (*o*-Ar-C), 61.7 (NCH_2), 32.8 (NCH_2CH_2), 32.1 (SCH_2CH_2), 28.7 (SCH_2CH_2). IR (KBr), ν (cm^{-1}): 1638 (s, C═N).

323. Yield: 6.5 g (10.6 mmol; 67.2%). MS (FAB$^+$, NOBA), *m*/*z*: 613 (10) [M$^+$ + 1]. ^{1}H NMR (200 MHz, $CDCl_3$): δ 8.30 (s, 4H, NCH), 7.75 (s, 8H, Ar-H), 3.72 (t, 8H, NCH_2), 2.62 (s, 8H, SCH_2), 2.52 (t, 8H, $NCH_2CH_2CH_2$), 1.95 (p, 8H, NCH_2CH_2). ^{13}C NMR (50.3 MHz, $CDCl_3$): δ 160.9 (NCH), 138.0 (Ar-*C*-CHN), 128.3 (*o*-Ar-C), 60.0 (NCH_2), 32.8, 30.5 and 29.8 ($NCH_2CH_2CH_2SCH_2$). IR (KBr), ν (cm^{-1}): 1639 (s, C═N).

The dicopper(I) compounds were prepared under Ar (standard Schlenk techniques), using degassed and water-free solvents. An excess (approximately 120%) of freshly prepared $[Cu(CH_3CN)_4]ClO_4$ in acetonitrile[15] was slowly added (1 h) to a stirred solution (CH_3CN/CH_2Cl_2 (1:1), 200 mL) of the macrocyclic ligands (0.34 mmol). Filtration yielded a yellow/orange to red/brown solution from which the complexes crystallized after reduction of the volume (ambient temperature, vacuum) to 50 mL. These products are air-stable, and the excess copper(I), oxidized to copper(II) was removed by washing the dicopper(I) compounds with acetonitrile.

[Cu$_2$242](ClO$_4$)$_2$. Yield: 144 mg (0.154 mmol; 45.2%). Calcd for $C_{32}H_{46}Cl_2Cu_2N_4O_9S_4$ (956.82): C, 40.16; H, 4.84; N, 5.85; S, 13.40; Cl, 7.41. Found: C, 40.20; H, 4.84; N, 5.99; S, 13.81; Cl, 7.46. MS (FAB$^+$, NOBA), *m*/*z*: 940 (4) [M$^+$], 839 (100) [M$^+$ − ClO_4], 738 (26) [M$^+$ − 2ClO_4], 675 (33) [M$^+$ − Cu$(ClO_4)_2$], 307 (93) [$C_{10}H_{20}N_2S_2^+$]. ^{1}H NMR (200 MHz, CD_3CN): δ = 8.59 (s, 4H, NCH), 7.37 (s, 8H, Ar-H), 4.03 (t, 8H, NCH_2), 3.17 (t, 8H, NCH_2CH_2), 3.06 (t, 8H, SCH_2), 2.07 (t, 8H, SCH_2CH_2). ^{13}C NMR (50.3 MHz, CD_3CN): δ 166.9 (NCH), 137.8 (Ar-*C*-CHN), 128.2 (*o*-Ar-C), 62.4 (NCH_2), 38.4 (NCH_2CH_2), 35.9 (SCH_2), 29.1 (SCH_2CH_2). IR (KBr), ν (cm^{-1}): 2922 (CH_2),1639 (s, C═N), 1091 (ClO_4^-).

[Cu$_2$323](ClO$_4$)$_2$. Yield: 146 mg (0.143 mmol; 42.0%). ^{1}H NMR (200 MHz, CD_3CN): δ 8.38 + 8.31 (s, 4H, NCH), 7.98 + 7.87 (pseudo-singulet, 8H, Ar-H), 3.73 (t, 8H, NCH_2), 2.96 (s, 8H, SCH_2), 2.73 (t, 8H, $NCH_2CH_2CH_2$), 2.00 (pseudo-singulet, 8H, NCH_2CH_2). ^{13}C NMR (50.3 MHz, CD_3CN): δ 164.5 (NCH), 138.6 (Ar-*C*-CHN), 129.7 (*o*-Ar-C), 62.7 (NCH_2), 35.0 ($NCH_2CH_2CH_2$), 33.4 (SCH_2), 30.4 (NCH_2CH_2). IR (KBr), ν (cm^{-1}): 2838−2926 (CH_2),1638 (s, C═N), 1625 (s, C═N), 1094 (ClO_4^-).

[Cu$_2$222-Me](ClO$_4$)$_2$. Yield: 138 mg (0.133 mmol; 39.0%). Calcd for $C_{36}H_{50}Cl_2Cu_2N_6O_8S_4$ (1037.06): C, 41.67; H, 4.85; N, 7.17; S, 13.09. Found: C, 41.45; H, 4.91; N, 7.50; S, 12.83. ^{1}H NMR (200 MHz, CD_3CN): δ 8.79 (s, 4H, NCH), 7.51 (s, 4H, Ar-H), 3.89 (t, 8H, NCH_2), 3.08 (s, 8H, SCH_2), 3.07 (t, 8H, NCH_2CH_2), 2.18 (s, 12H, CH_3). ^{13}C NMR (50.3 MHz, CD_3CN): δ 164.7 (NCH), 136.9 (Ar-*C*-CHN), 129.0 (*o*-Ar-C), 58.9 (NCH_2), 34.6 (NCH_2CH_2), 33.1 (SCH_2), 18.7 (CH_3).

[Cu$_2$222-OMe](ClO$_4$)$_2$. Yield: 130 mg (0.147 mmol; 43.0%). Calcd for $C_{32}H_{44}Cl_2Cu_2N_4O_{12}S_4$ (1037.06): C, 38.40; H, 4.43; N, 5.60; S, 12.79. Found: C, 38.72; H, 4.44; N, 6.02; S, 12.54. ^{1}H NMR (300 MHz, CD_3CN): δ 8.78 (s, 4H, NCH), 7.17 (s, 4H, Ar-H), 3.94 (t, 8H, NCH_2), 3.63 (s, 12H, OCH_3), 3.10 (s, 8H, SCH_2), 2.95 (t, 8H, NCH_2CH_2). ^{13}C NMR (75.5 MHz, CD_3CN): δ 163.9 (NCH), 153.9 (Ar-*C*-OCH_3), 127.9 (Ar-*C*-CHN), 110.4 (Ar-CH), 59.7 (NCH_2), 56.9 (OCH_3), 34.5 (NCH_2CH_2), 33.5 (SCH_2). IR (KBr), ν (cm^{-1}): 1616 (s, C═N), 1088 (s, ClO_4^-).

(14) Hay, R. W.; Gidney, P. M. *J. Chem. Soc., Dalton Trans.* **1975**, 779.

(15) v. Rijn, J.; Reedijk, J. *J. Chem. Soc., Dalton Trans.* **1987**, 2579.

222-phane. To a stirred solution (Ar; ambient temperature) of isomerically pure *trans*-4,7,13,16-tetrabrom[2.2]paracyclophane[6] (9.70 g, 18 mmol) in dry ether (300 mL) was added dropwise a solution of *n*-butyllithium (20% in hexane; 48.0 g, 0.148 mol). A solution of dry DMF (11.1 g, 0.148 mol) in dry ether (200 mL) was added after 6 h. This was left overnight (stirring; Ar; 25 °C), and then water (100 mL) was added. The organic phase was recovered, washed with water (4 × 200 mL), and dried ($Mg(SO_4)$), and the solvent was evaporated under reduced pressure. Recrystallization from $CHCl_3$/petroleum ether 60/70 (1:1) produced a yellowish solid (2 g; mixture (GC−MS) of 77% tetraformylparacyclophane, 17% triformylparacyclophane, 6% dibromdiformylparacyclophane). Further recrystallization produced the pure tetraformylparacyclophane. Yield: 1.2 g (3.1 mmol; 20%). Calcd for $C_{16}H_{22}O_5$ (328.1): C, 71.02; H, 5.37. Found: C, 71.65; H, 5.57. ^{1}H NMR (200.1 MHz, $CDCl_3$): δ 9.96 (s, 4H, C*H*O), 6.99 (s, 4H, Ar-*H*); 4.08−4.25 (m, 4H, CH_2)); 3.04−3.20 (m, 4H, CH_2). ^{13}C NMR (50.3 MHz, $CDCl_3$): δ 191.1 (CHO), 143.0 (Ar-*C*-CHO), 139.4 (Ar-*C*-CH_2), 137.8 (Ar-*CH*), 33.2 (Ar-C-*C*H_2). IR (KBr), υ (cm^{-1}): 1686 (s, C═O).

To a stirred solution of 1,8-diamino-3,6-dithiooctane (360 mg; 2.0 mmol; in CH_3CN, 300 mL) is slowly added (3 h) the tetraformylparacyclophane (320 mg; 1.0 mmol; in CH_3CN/toluene (1:1), 200 mL). After stirring overnight, side products are removed by filtration, and the solvent is evaporated under reduced pressure to afford the yellowish product. Yield: 400 mg (0.7 mmol; 66%). Calcd for $C_{32}H_{40}N_4S_4$ (608.9): C, 63.14; H, 6.63; N, 9.21; S, 21.03. Found: C, 62.35; H, 6.55; N, 8.54; S, 20.39. MS (FAB$^+$, NOBA), *m*/*z*: 609 (100) [M$^+$]. ^{1}H NMR (200.1 MHz, $CDCl_3$): δ 8.25 (s, 4H, NC*H*), 7.08 (s, 4H, Ar-H), 2.5−4.5 (m, 32H, aliphatic H's; poorly resolved (very small solubility)). IR (KBr), υ (cm^{-1}): 1636 (s, C═N).

[$Cu_2$222-phane](ClO_4)$_2$. Due to solubility problems the dicopper(I) compound of the helical ligand was prepared directly from the reaction mixture of 222-phane (see above, synthesis under Ar and with degassed, water-free solvents). To the stirred solution of the ligand (400 mg; 0.7 mmol) in CH_3CN/toluol 4:1 (500 mL) was added dropwise $[Cu(CH_3CN)_4]ClO_4$ (in CH_3CN, 16 mL; 0.077 mmol/L).[15] The yellow-orange solution was filtrated after 1 h and reduced to 50 mL by rotary evaporation at ambient temperature. To obtain single crystals, further evaporation of the solvent produced additional solid product. Yield: 350 mg (0.3 mmol; 52%). Calcd for $C_{32}H_{40}Cl_2Cu_2N_4O_8S_4 \cdot 0.5H_2O \cdot 0.5CH_3CN$ (952.9): C, 40.73; H, 4.47; N, 6.58; S, 13.30. Found: C, 39.94; H, 4.60; N, 6.71; S, 13.29. ^{1}H NMR (300.1 MHz, CD_3NO_2): δ 8.84 (s, 4H, NC*H*), 7.72 (s, 4H, Ar-H), 3.75 (d, 4H, $^2J_{AX}$ = 9.8 Hz, SCH_2), 2.61 (d, 4H, $^2J_{AX}$ = 9.8 Hz, SCH_2, $\Delta\nu$ = 341.3 Hz), 3.66 (dd, 4H, $^2J_{AX}$ = 5.7 Hz, $^4J_{HH}$ = 4.7 Hz, Ar-C-CH_2), 2.84 (dd, 4H, $^2J_{AX}$ = 5.7 Hz, $^4J_{HH}$ = 4.7 Hz, Ar-C-CH_2, $\Delta\nu$ = 248.1 Hz), 4.13 (dd, 4H, $^2J_{AX}$ = 13.4 Hz, $^3J_{HH}$ = 4.1 Hz, NCH_2), 3.39 (dd, 4H, $^2J_{AX}$ = 14.7 Hz, $^3J_{HH}$ = 2.8 Hz, NCH_2, $\Delta\nu$ = 223.3 Hz), 4.01 (mt, 4H, $^2J_{AX}$ = 12.5 Hz, NCH_2CH_2), 3.16 (dt, 4H, $^2J_{AX}$ = 13.7 Hz, $^3J_{HH}$ = 4.9 Hz, NCH_2CH_2, $\Delta\nu$ = 257.2 Hz). IR (KBr), υ (cm^{-1}): 1622 (s, C═N), 1092 (s, Cl−O).

Single crystals of all the dicopper(I) compounds, suitable for X-ray measurements, were obtained from concentrated solutions of the compounds at room temperature.

Crystallography. Cell constants were determined by least-squares fits to the setting parameters of 25 independent reflections, measured and refined on a Rigaku AFC7R diffractometer or an Enraf-Nonius CAD4-F diffractometer. The crystallographic data are summarized in Table 1. Data reduction and application of Lorentz, polarization, and ψ scan and analytical absorption corrections were carried out using teXsan.[16] The structures were solved by direct methods using SHELXS-86[17] and refined using full-matrix least-squares methods with teXsan.[16] Hydrogen atoms were included at calculated sites with thermal parameters derived from the parent atoms. Non-hydrogen atoms were refined anisotropically. Scattering factors and anomalous dispersion terms for Cu (neutral atoms) were taken from International Tables.[17] Anomalous dispersion effects were included in F_c;[18] the values for $\Delta f'$ and $\Delta f''$ were those of Creagh and McAuley.[19] The values for the mass attenuation coefficients are those of Creagh and Hubbell.[20] All other calculations were performed using teXsan.[16]

Acknowledgment. Generous financial support by the German Science Foundation (DFG) and the Fonds of the Chemical Industry (FCI) is gratefully acknowledged. This project has also been supported by a DAAD/ARC grant.

Supporting Information Available: Listings of atom coordinates, anisotropic thermal parameters, close intermolecular contacts, torsion angles, details of least-squares planes calculations, and observed and calculated structure factor amplitudes have been deposited and are available on the Internet only. Access information is given on any current masthead page.

IC980216Q

(16) *TeXsan Structure Analysis Software*; Molecular Structure Corp.: The Woodlands, TX; 1995.
(17) Sheldrick, G. M. *SHELX-76: A Program for X-Ray Crystal Structure Determination*; University of Cambridge: England, 1976.
(18) Cromer, D. T.; Waber, J. T. *International Tables for X-Ray Crystallography*; The Kynoch Press: Birmingham, England, 1974; Vol. IV.
(19) Creagh, D. C.; McAuley, W. J. *International Tables for Crystallography*; Wilson, A. J. C., Ed.; Kluwer Academic Publishers: Boston, 1992; Vol. C, Table 4.2.6.8, pp 219−222.
(20) Creagh, D. C.; Hubbell, J. H. *International Tables for Crystallography*; Wilson, A. J. C., Ed.; Kluwer Academic Publishers: Boston, 1992; Vol. C, Table 4.2.4.3, pp 200−206.